Genetically-determined variations in photosynthesis indicate roles for specific fatty acid species in chilling responses

Authors

Donghee Hoh[1,2], Patrick J. Horn[3], Atsuko Kanazawa[1,4], John Froehilch[1], Jeffrey Cruz[1], Oliver L Tessmer[1], David Hall[1], Lina Yin[6], Christoph Benning[1,5,7] and David M. Kramer [1,5*]

Affiliations

[1] MSU-DOE Plant Research Laboratory, [2] Cell & Molecular Biology Program, Michigan State University, [3] Department of Biology, East Carolina University, Greenville, NC USA [4] Department of Chemistry, [5] Department of Biochemistry and Molecular Biology, Michigan State University, [6] Department of Biology, Northwest A&F University, China, [7] Department of Plant Biology, Michigan State University, East Lansing, MI 48824 USA,

*Corresponding Author

Keywords

phosphatidylglycerol (PG), PG 16:1$^{\Delta 3trans}$, Photosynthesis, Natural Variation, Quantitative Trait Loci (QTL), Chilling stress (Low temperature stress), Cowpea

Summary Statement

Analyses of natural variation in lipid contents suggest that natural variations in chilling photosynthetic responses in cowpea are modulated by specific fatty acid species, e.g., the thylakoid phosphatidylglycerol 16:1$^{\Delta 3trans}$, rather than bulk lipid properties, e.g., unsaturation levels.

Abstract

Using a population of recombinant inbred lines (RILs) cowpea (*Vigna unguiculata.* L. Walp), we tested for co-linkages between lipid contents and chilling responses of photosynthesis. Under low temperature conditions (19°C/13°C, day/night), we observed co-linkages between quantitative trait loci (QTL) intervals for photosynthetic light reactions and specific fatty acids, most strikingly, the thylakoid-specific fatty acid $16:1^{\Delta 3trans}$ found exclusively in phosphatidylglycerol (PG 16:1t). By contrast, we did not observe co-associations with bulk polyunsaturated fatty acids or high-melting-point-PG (sum of PG 16:0, PG 18:0 PG 16:1t) previously thought to be involved in chilling sensitivity. These results suggest that in cowpea, chilling sensitivity is modulated by specific lipid interactions rather than bulk properties. We were able to recapitulate the predicted impact of PG 16:1t levels on photosynthetic responses at low temperature using mutants and transgenic *Arabidopsis* lines. Because PG 16:1t synthesis requires the activity of peroxiredoxin-Q, which is activated by H_2O_2 and known to be involved in redox signaling, we hypothesize that the accumulation of PG 16:1t occurs as a result of upstream effects on photosynthesis that alter redox status and production of reactive oxygen species.

Introduction

The chloroplast thylakoid membrane, which houses the central complexes catalyzing the light reactions, contains a set of lipids that is distinct from other cellular components, and differences in the thylakoid lipid profile have been linked to specific environmental responses (Hurlock, Roston, Wang & Benning 2014; Cook, Lupette & Benning 2021; Yu, Zhou, Fan, Shanklin & Xu 2021). It has been proposed that changes in thylakoid lipid compositions, and in particular the balance of fatty acid (FA) saturation and unsaturation of membrane lipids, influence viability and photosynthetic capacity in response to chilling temperature (Hugly & Somerville 1992; Miquel, James, Dooner & Browse 1993; Wu, Lightner & Warwick 1997), leading to the hypothesis that a reduced poly-unsaturation level contributes to chilling sensitivity, while the opposite is proposed to limit heat tolerance.

However, this view remains to be thoroughly tested, and while in some cases clear correlations have been reported between the loss of specific classes of lipids and tolerance to low temperatures, this is not always the case. Here, we revisit two classic hypotheses: 1) a reduced poly-unsaturation level contributes to chilling sensitivity and 2) that specific species of PGs, high-melting-point phosphatidylglycerol (HMP-PG), confer chilling sensitivity.

In support of the poly-unsaturation hypothesis, some *Arabidopsis* mutants (e.g., *fad6* and *fad2*) with lower ratios of unsaturated: saturated FAs showed reduced photosynthetic activity at low temperature. The *Arabidopsis fad6* mutant (deficient in chloroplast omega 6 desaturase activity), which shows reduced levels of the

polyunsaturated acyl groups 16:3 and 18:3 (carbons : double bonds), was indistinguishable in appearance from wild type at 22 °C, but became chlorotic after 3 weeks exposure to low temperature (5°C) (Hugly & Somerville 1992). In an *Arabidopsis fad2* mutant, which has reduced levels of polyunsaturated phosphatidylcholine (PC) containing 18:3 due to a deficiency in delta 12 desaturase activity within the endoplasmic reticulum, no distinctive phenotype was observed at 22°C, whereas *fad2* plants died after 7 weeks at 6°C (Miquel *et al.* 1993). Notably, the composition of poly-unsaturated FAs (e.g., trienoic 16:3 or 18:3 versus dienoic 16:2 or 18:2) is linked to chilling sensitivity in *Arabidopsis*. In higher-order mutants that decreased the levels of trienoic FA (but maintained similar levels of overall poly-unsaturated to saturated FA as wildtype), long-term growth at 4°C resulted in comparatively poor photosynthetic performance and impaired chloroplast ultrastructure relative to wild-type plants demonstrating the importance of trienoic FAs (Routaboul, Fischer & Browse 2000). Despite this genetic evidence linking poly-unsaturation levels and chilling sensitivity, in higher-order mutants where acyl chain length is altered in addition to poly-unsaturation levels the photosynthetic performance-chilling associations become more complex (Barkan, Vijayan, Carlsson, Mekhedov & Browse 2006). For example, a suppressor screen of *fab1* (a mutant line that alters the ratio of 16C : 18C fatty acids through a disruption of plastid beta-ketoacyl-ACP synthase II) produced a line with increased lipid saturation but improved photosynthetic performance at low temperature (Barkan *et al.* 2006). One suppressor contained an allele of FAD5, which codes for a chloroplast delta 7 desaturase that acts on a 16C FA that is specifically esterified at the *sn*-2 position of

monogalactosyldiacylglycerol (MGDG) (Kunst, Browse & Somerville 1989), leading to a loss of 16:3 and increased lipid saturation.

An alternative hypothesis is that specific species of phosphatidylglycerol (PG), high-melting-point PG (HMP-PG), e.g., molecules that contain only 16:0, 16:1$^{\Delta 3trans}$ (PG 16:1t), and 18:0 fatty acids confer chilling sensitivity (Murata, Sato, Takahashi, Hamazaki & Cell Physiology 1982; Murata 1983; Murata & Yamaya 1984; Roughan 1985; Murata & Nishida 1990). Starting from the early 1970s, it has been suggested that the primary event of chilling sensitivity is a thermal transition, liquid-crystalline phase to gel phase, in the cellular membrane and that molecular species of chloroplast HMP-PG contribute to chilling sensitivity. This hypothesis is supported by the liquid-crystalline phase to gel phase transitions observed only in chilling-sensitive but not in chilling-resistant plants (Murata *et al.* 1982; Murata 1983; Murata & Yamaya 1984; Roughan 1985; Murata & Nishida 1990). Other studies supporting this hypothesis show the correlation between chilling sensitivity and the percentage of HMP-PG molecular species by surveying 74 plant species (Murata *et al.* 1982; Murata 1983; Murata & Yamaya 1984; Roughan 1985; Murata & Nishida 1990). As a follow up to studies in the 1980s, changes in the level of HMP-PGs in transgenic plants and mutants were pursued in the 1990s (Wolter, Schmidt & Heinz 1992; Wu & Browse 1995). As an example, Wolter et al. showed that increasing HMP-PG to more than 50% led to chilling sensitivity (Wolter *et al.* 1992). However, a contrary result has also been reported, demonstrating that an increased fraction of HMP-PG in *fab1*, which has a higher PG 16:0 content, did not confer chilling sensitivity, concluding that the high-melting-point

molecular species of PG cannot be a primary determinant of chilling sensitivity (Wu & Browse 1995).

Collectively, the complex phenotypes within these studies suggest that the impact of lipid changes may be governed by specific lipid interactions with protein complexes, rather than bulk physico-chemical properties (Barkan *et al.* 2006), leaving the exact mechanisms by which specific lipids or FAs affect photosynthesis and chilling sensitivity an open question (Siegenthaler & Murata 2006). Indeed, the thylakoid membrane is composed of a complex mixture of lipids, protein complexes (Pribil, Labs & Leister 2014), and lipid-soluble components such as quinones (Anderson 1986) that can interact in complex ways. Thus, it may not be possible to draw straightforward conclusions about the roles of lipids based simply on their bulk physico-chemical properties in defined mixtures. Indeed, there is direct and indirect evidence for specific interactions between certain lipid components and specific photosynthetic complexes (Dörmann, Hoffmann-Benning, Balbo & Benning 1995; Reifarth *et al.* 1997; Härtel, Lokstein, Dörmann, Grimm & Benning 1997; Xu *et al.* 2002; Hagio *et al.* 2002; Babiychuk *et al.* 2003; Yu & Benning 2003; Steffen, Kelly, Huyer, Dörmann & Renger 2005; Guo *et al.* 2005; Hölzl *et al.* 2006, 2009; Ivanov *et al.* 2006; Kobayashi, Kondo, Fukuda, Nishimura & Ohta 2007; Kobayashi *et al.* 2013; Aronsson *et al.* 2008; Wu *et al.* 2013; Fujii, Kobayashi, Nakamura & Wada 2014). It is also clear that the loss of one lipid component may be compensated by changes in composition through the up- or down-regulation of complex, integrated lipid metabolism pathways (Li-Beisson *et al.* 2013). The mechanism by which such compensation occurs is not clear. Moreover, it is

also possible that loss-of-function mutations might have a strong impact only under specific sets of conditions not typically imposed in the laboratory.

Recently, high-throughput phenotyping (Hoh *et al.* 2021) was applied to a recombinant inbred line (RIL) population of *Vigna unguiculata* L. Walp (cowpea), exhibiting large variations in chilling sensitivity. Cowpea is a warm-climate species and has a high level of genetic diversity (Huynh *et al.* 2018), allowing us to probe natural variations in chilling stress that might be distinct from those in more chilling tolerant species such as *Arabidopsis.* A range of possible mechanistic bases for these variations was explored by assessing co-segregation (or lack thereof) between genetic diversity and multiple traits by taking advantage of advanced high-throughput phenotyping tools. It was found that genetic loci which affect the primary reactions of photosynthesis that involve redox states of Q_A, establishment of the thylakoid proton motive force (*pmf*) through effects on cyclic electron flow (CEF), and subsequent acidification of the thylakoid lumen led to differences in the rates of photodamage to PSII. Here, we asked the question whether these interactions could be associated with changes in lipid composition. To accomplish this, we measured variations in FA compositions across the RIL population, allowing us to test for potential linkages among photosynthetic processes and lipid molecular species with varying characteristics. Our data suggest that PG 16:1t, but not other species of HMP-PG, was negatively associated with the robustness of photosynthesis. We qualitatively recapitulated these phenomena in a series of mutants of *Arabidopsis* with differences in PG 16:1t contents. The results showed qualitatively similar effects, supporting a role of PG 16:1t in contributing to

chilling sensitivity in both cowpea and *Arabidopsis*.

Material and Methods

Plant materials, growth and experimental conditions.

Cowpea genotypes and growth conditions.

Cowpea genotypes (CB27 and 24-125B) were as described in (Hoh *et al*. 2021). Seedlings at the “VC” stage (4 d after seed germination, https://beanipm.pbgworks.org/cowpea) were transferred from the staging chamber to the DEPI chamber (Figure S1). The light intensity was changed in a sinusoidal pattern at 30 min intervals over the course of a 14 h day with the highest light intensity (500 µmol m^{-2} s^{-1}) occurring midday. The lowest light intensity (50 µmol m^{-2} s^{-1}) was at the beginning and end of the day. For the detailed light intensity changes, see Figure S1B. On Day 1, as the control for the low temperature (LT) experiment, plants were kept under the mentioned lighting conditions at 29°C/19°C (control temperature: CT). After Day 1, plants were subjected to temperatures of 19°C/13°C for 3 days for the low temperature treatment (low temperature: LT) (Figure S1A).

Arabidopsis mutants with altered fatty acid composition.

Wild type *Arabidopsis thaliana* ecotypes Columbia-0 (Col-0) and Columbia-2 (Col-2), as well as fatty acid desaturase 4 (FAD4) (locus *AT4G27030*) knockout (KO) (Alonso *et al.* 2003; Gao *et al.* 2009) and overexpression (OX) lines (by adding *pMDC85-FAD4*) were

used in this study. FAD4 is a desaturase required for the synthesis of 16:1t at the *sn*-2 position of PG (Gao *et al.* 2009). Overexpression lines in the pMDC binary vector system (Curtis & Grossniklaus 2003) were generated as described previously (Horn, Smith, Clark, Froehlich & Benning 2020) using the FAD4 coding sequence.

Arabidopsis growth conditions.

Arabidopsis seeds were planted in Redi-earth soil (Hummert Cat. # 10-2030-1) and stratified at 5°C for 3 days and grown under 100 µmol photons m^{-2} s^{-1} light cool fluorescent lights 16h: 8h day: night cycle at constant 21°C, 60% relative humidity. The 16-day-old plants were moved to DEPI chambers and exposed to an actinic light intensity regime similar to that of the cowpea experiments, every 30 minutes with a pattern based on sinusoidal curve and a peak intensity of 500 µmol photons m^{-2} s^{-1} except that the light/dark pattern was 16/8 hours and that, on Day 1, the daytime temperature was set to 21°C and decreased to 6°C on Day 2 for measurements under chilling stress.

Photosynthetic phenotyping.

Chlorophyll fluorescence imaging was performed using Dynamic Environmental Phenotype Imager (DEPI) chambers (Cruz *et al.* 2016), with modifications described in (Tietz, Hall, Cruz & Kramer 2017). Detailed experimental procedures were performed as described in Hoh *et al.* (2021).

Polar glycerolipid profiling of cowpea population.

Polar lipid contents were determined for each of the cowpea RIL accessions using the methods described previously (Wang & Benning 2011). Samples were collected following the three-day experiments, so that the results should reflect chilling-induced lipid profiles. Lipid was extracted from fresh leaves with the solvent composed of methanol, chloroform and formic acid (20:10:1, v/v/v) followed by 0.2 M phosphoric acid (H_3PO_4) and 1 M KCl buffer. Lipid classes were separated by thin layer chromatography (TLC) using a mobile phase of (acetone: toluene: water 91:30:7.5 mL), followed by brief iodine staining and isolation of silica of bands representing monogalactosyldiacylglycerol (MGDG), digalactosyldiacylglycerol (DGDG), sulfoquinovosyldiacylglycerol (SQDG), phosphatidylcholine (PC), phosphatidylglycerol (PG), and a combination of phosphatidylethanolamine (PE) and phosphatidylinositol (PI) (hereafter referred to as PEPI). Third, fatty acyl methyl esters (FAMEs) were produced from the lipids with 1 N hydrochloric acid (HCl) in anhydrous methanol and pentadecanoic acid (15:0) as internal standard by incubating in an 80°C water bath for 25 min. Fourth, gas-liquid chromatography together with flame ionization detection (GLC-FID) was used for analysis of FAMEs. FAME contents were normalized using an internal standard. The mole fractions for FAME species were calculated by normalizing to the estimated sum for all lipid species, accounting for differences in acyl chain length and unsaturation response factors.

Linkage analysis and QTL mapping.

Analyses of QTL associations were performed as described in Hoh *et al.* (2021) using single nucleotide polymorphism (SNP) markers for genotype data of CB27 x 24-125B-1, which were obtained from (Lonardi *et al.* 2019) based on EST sequences produced by (Muchero *et al.* 2009). The construction of the linkage-map was performed as described in Hoh *et al.* (2021). QTL analysis was conducted using the Multiple QTL Mapping (MQM) model (genome scan with multiple QTL models) in the R/qtl package (Broman & Sen 2009). Levels of significance were determined by the number of permutations set at 1000 and a nominal significance cutoff of $p < 0.05$ over all replicates. More details of the analysis and candidate gene prediction are described in Hoh *et al.* (2021).

Results and Discussion

Temperature effects on lipid profiles for parent lines.

RIL population parent lines, CB27 and 24-125B-1, were chosen based on differential sensitivity to temperature, as described in Hoh *et al.* (2021). The two lines showed only small differences in photosynthetic phenotypes under the control temperature (CT, 29°C/19°C, day/night) but large differences under low temperature (LT, 19°C/13°C). CB27 had higher tolerance (relatively high photosynthetic efficiency (Φ_{II}) and low photoinhibition) while 24-125B had a lower tolerance (strong decreases in Φ_{II} and large increases in photoinhibition). To determine conditions under which significant

differences between genotypes are most likely to be apparent, we performed lipid profiling of two parents of RILs under three different conditions, control temperature (CT), 2nd day (LT 2d) or third day of (LT 3d) of low temperature (LT) conditions.

Relative abundances of lipid classes

Figures S2 and S3 compare the relative abundances for polar lipid classes, as well as the ratios of DGDG/MGDG, the two galactolipids of the photosynthetic membrane. (For clairy we present the data in two ways: Figure S2 compares the two genotypes, while Figure S3 compares dependencies on condition for each genotype). Under CT, CB27 showed a significantly higher proportion in MGDG and SQDG, with corresponding lower amounts of DGDG and a combination of PE and PI (PEPI) compared to 24-125B-1 ($p<0.05$), whereas no significant differences were observed for the other lipid classes (Figure S2A). Upon exposure to LT, increased SQDG levels were observed in 24-125B-1, whereas levels in CB27 remained similar (Figure S3A). In contrast, exposure to LT led to significantly decreased MGDG and increased DGDG content in CB27, effectively increasing the DGDG/MGDG ratio from 0.43 at CT to 0.72 at LT 3d ($p<0.05$, Figure S3B). Furthermore, the DGDG/MGDG ratios in 24-125B-1 remained similar during LT treatment, although initial DGDG/MGDG ratios were higher compared to CB27 on CT on Day 1 ($p<0.05$) (Figure S3B). It should be noted that this pattern of changes in CB27 was qualitatively similar to that observed by (Moellering, Muthan & Benning 2010). That is, although freezing at -2 °C, but not chilling conditions were

applied, DGDG levels increased and MGDG levels decreased as driven by the action of SFR2, a processive galactolipid galactosyltransferase.

Relative fatty acid compositions

Figure S4 shows the relative composition of fatty acids for each lipid class for two parental lines under CT, LT 2d and LT 3d. Note, cowpea is an 18:3 plant and does not produce 16:3 FA, a common marker of plastid lipids for many plants like *Arabidopsis* (Mongrand, Bessoule, Cabantous & Cassagne 1998). Under CT, the acyl composition was similar for most molecular species, including MGDG and DGDG, between the sensitive line (24-125B-1) and tolerant line (CB27) (Figure S4A and D). However, in PG, 16:1t content was significantly higher and 18:3 significantly lower in CB27 relative to 24-125B-1 (Figure S4G). Additional differences were observed in SQDG and PEPI including lower levels of 16:0, 18:0 and higher levels of 18:2 in CB27 relative to 24-125B-1 (Figure S4J, S4P).

There were minor changes in FA composition within all lipid classes under LT treatment (Figure S4, S5). However, significant shifts in PG composition were particularly notable (Figure S5C). In CB27, LT treatment led to significant decreases in PG containing 16:0, 16:1t, and 18:0 with a corresponding significant increase in 18:3 (and while not statistically significant, a general increase in 18:2 as well). In contrast, 24-125B-1 showed a more complex phenotype that can generally be viewed as the opposite to

CB27. There was a clear, significant increase in 16:1t and decrease in 18:0, with a likely decrease in 18:3 (at least at LT 2d). Figure 1 shows HMP-PG (summed 16:0, 16:1t, and 18:0) for two parental lines in three temperature conditions in order to verify the HMP-PG hypothesis, which posits that the combination of saturated fatty acid (16:0 and 18:0) or 16:1t contributes to chilling sensitivity (Raison 1973; Lyons 1973; Murata & Yamaya 1984; Roughan 1985). Compared to CT, the chilling tolerant CB27 line showed decreases in HMP-PG ($p<0.05$) on Day 2 and 3, the first and second days of LT (Figure 1). By contrast, the chilling sensitive 24-125B-1 line had increased HMP-PG on Day 2 (first day of LT) ($p<0.05$), but no significant differences on the third day of LT (Figure 1). This result is partially consistent with a transient involvement of HMP-PG in chilling sensitivity. However, there is no significant difference ($p>0.05$) in HMP-PG between the lines in LT 2d and 3d (see Figure S6B and 6C, which compare the data with different significance tests), suggesting that rather than the sum of HMP-PG content, specific fatty acid content could affect chilling sensitivity. To tease apart the effect of specific fatty acid content, each FA composition and HMP-PG was analyzed for QTL associations separately (see below).

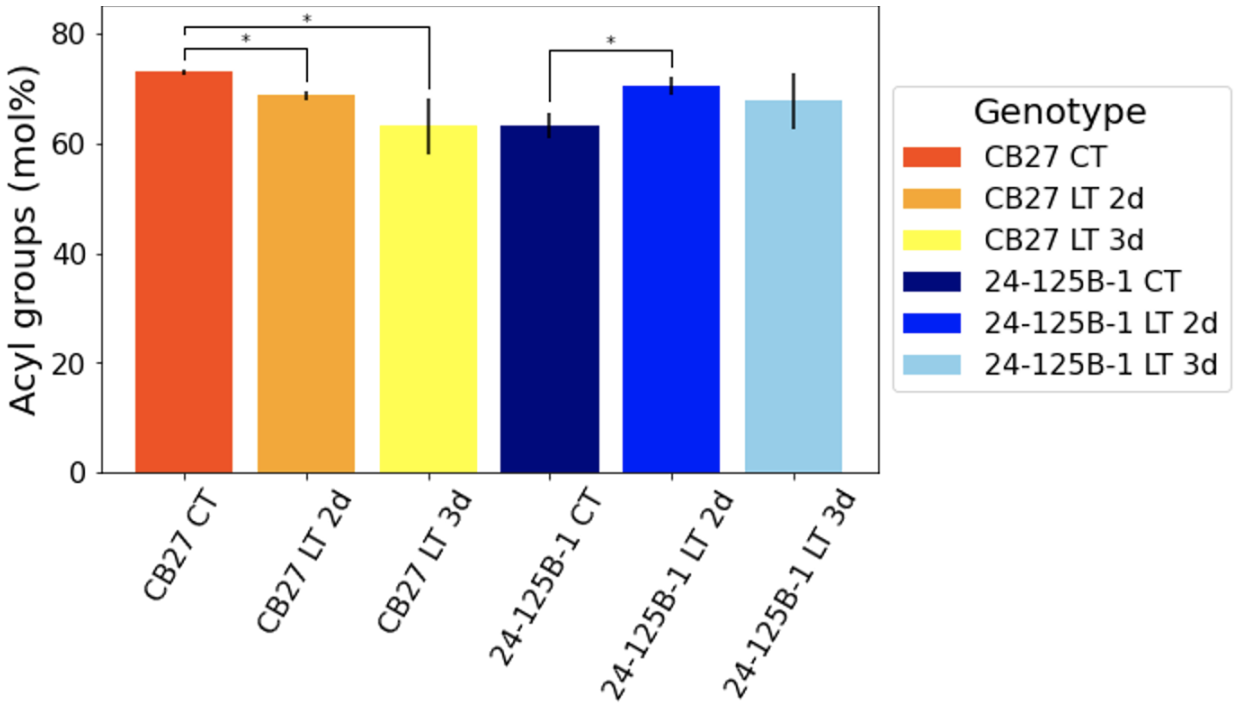

Figure 1. HMP-PG for two parental lines (CB27 and 24-125B-1) in three temperature conditions.
CT, control temperature; LT 2d, 2nd Day of low temperature; LT 3d 3rd Day of low temperature. HMP-PG is the total composition for molecular species of PG 16:0, 18:0 and PG 16:1t. The averaged replicates (n≥3) for each value are shown as a bar graph with error bar (SD). The asterisks show significant differences between the groups (as shown in brackets) from t-test ($p<0.05$). CB27 showed decreased HMP-PG after chilling treatment ($p<0.05$), but 24-125B-1 showed increased mol % ($p<0.05$ for LT 2d, n.s. for LT 3d).

Effects of chilling temperatures on lipid classes and fatty acid profiles for the diversity panel.

Based on lipid profiling for two parental lines (Figure 1 and Figure S3 and S4) and photosynthetic responses (Hoh *et al.* 2021), we chose the third day of LT for detailed lipid and fatty acid profiling over the entire RIL population.

Relative abundances of lipid classes

Figure S7 A-F shows histograms for relative abundance (mol %) of classes across genotypes. The two parent lines showed no significant differences in MGDG (34 ± 2, 31 ± 3), DGDG (25 ± 2, 23 ± 3) or PG (10.6 ±1.4, 11.9 ± 1) and SQDG (4.9 ± 0.9, 5.8 ± 0.7, (all with $p>0.05$) (Figure S7). However, the distributions of lipid class compositions for the progenies exceeded those between the two parent lines, showing larger ranges in the lipid class compositions relative to the parent lines. In particular, PC (Figure S7E) and PEPI (Figure S7F) showed much larger differences in average values in the progeny compared to the parent lines. Figure S7G indicates that although the DGDG/MGDG ratio was not significantly different between the parent lines (0.72 ± 0.05, 0.73 ± 0.08, $p>0.05$) there was a larger range (0.55 - 0.9) within the progeny lines.

Relative fatty acid compositions

Figure S8 shows histograms for FA compositions across the RIL population, with values for the parent lines indicated by color-coded arrows. Compared to 24-125B-1, CB27 showed significantly higher polyunsaturated fatty acid contents MGDG 18:2 (Figure S8B), DGDG 18:2 (Figure S8E) and PG 18:2 (Figure S8G) (all with $p<0.05$). The sensitive line, 24-125B-1, showed slightly higher, but barely significantly, saturated fatty acid MGDG 16:0 (Figure S8A). No significant differences ($p>0.05$) were seen between parent lines for DGDG 16:0 (Figure S8D), SQDG 16:0 (Figure S8I), SQDG 18:0 (Figure

S8J) and PEPI 16:0 (Figure S8R).

Figure 2A-D describes the distributions of compositions of selected fatty acids across the RIL population. Compared to CB27, 24-125B-1 had higher PG 16:1t (32.34 ± 2.66, 35.64 ± 1.96, $p<0.05$, Figure 2A), PG 18:0 (2.21 ±0.56, 2.92 ± 0.49, $p<0.05$, Figure 2B), but no significant differences for PG 16:0 (30.70 ± 3.85, 32.05 ± 3.51, $p>0.05$, Figure 2C) or PEPI 18:1 (2.80 ± 0.56, 2.13 ± 0.43, $p>0.05$, Figure 2D).

Despite the relatively small differences in lipid components between the parent lines, the progeny showed wider distributions of these components, which as discussed below showed significant associations with both photosynthetic phenotypes and genetic components. The correlation between each fatty acid content and Φ_{II} (taken from Hoh *et al.* 2021 c.f. Figure 1) from 1.5 h prior to the end of day 3 (206 µmol, m^{-2}, s^{-1}). Figures 2 E-H show that Φ_{II} is strongly negatively correlated with PG 16:1t (Figure 2E, $R^2 = 0.741$, $p<0.0001$), weakly (but still significantly) negatively correlated with PG 18:0 (Figure 2F, $R^2 = 0.126$, $p = 0.001$), and weakly positively correlated with PG 16:0 (Figure 2G, $R^2 = 0.063$, $p = 0.025$) and PEPI 18:1 (Figure 2H, $R^2 = 0.348$, $p < 0.0001$).

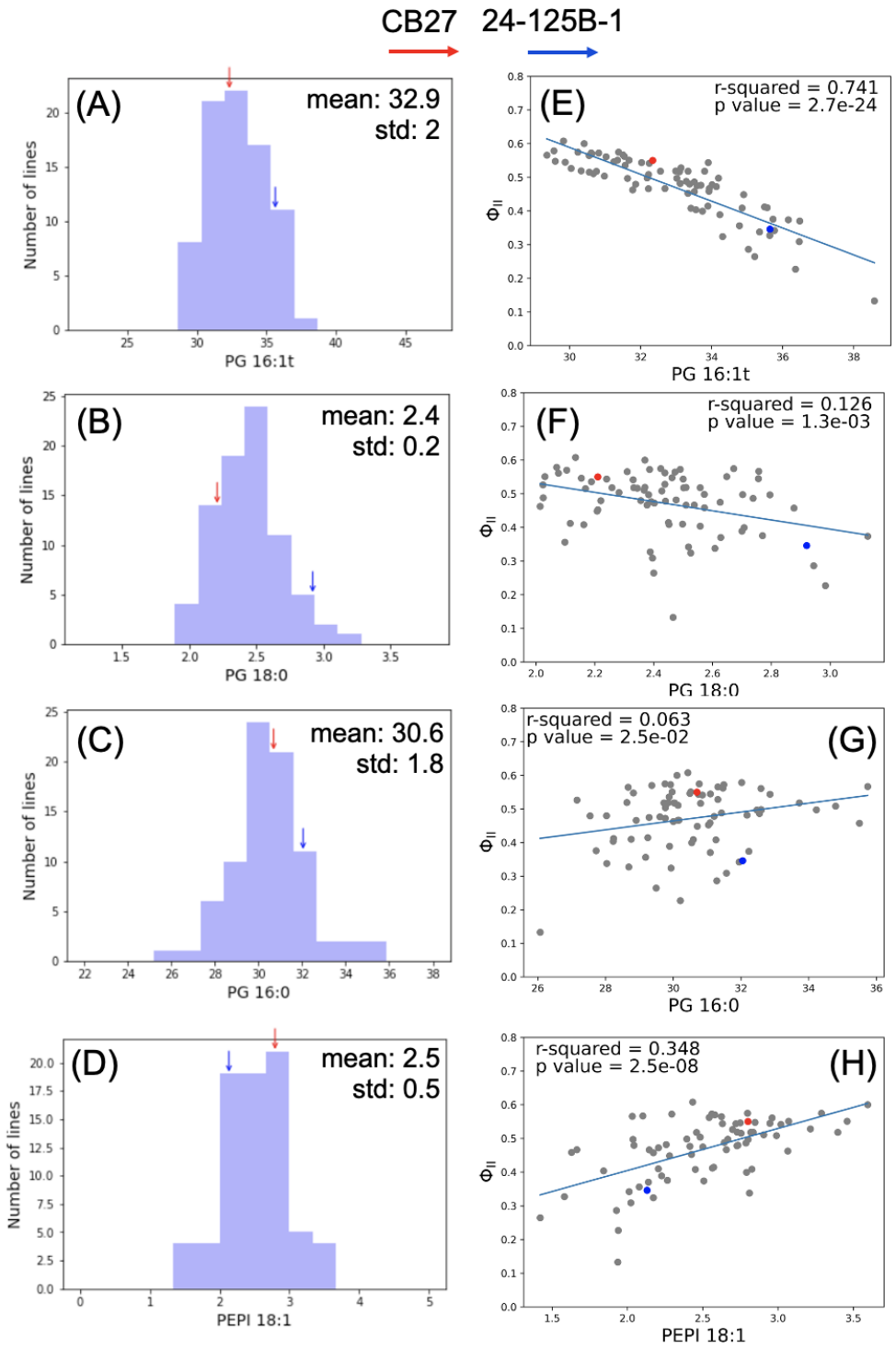

Figure 2. Histograms of the contents of selected fatty acids across genotypes (A: PG 16:1t, B:PG 18:0, C: PG 16:0, D: PEPI 18:1) and the correlation of selected fatty acids and PSII quantum efficiency (Φ_{II}) across the RIL lines in chilling condition

(E-H). (A-D) The averaged replicates (n≥3) for each phenotype value of RILs including two parental lines are shown as histograms. The mean and standard deviation of the population are shown above each histogram. The arrows indicate two parental lines (CB27, red; 24-125B-1, blue). (E-H) Correlation plot of selected fatty acids against Φ_{II} data from DEPI data, at 1.5 h prior to the end of Day 3 (206 µmol, m^{-2}, s^{-1}) for the RILs and parental lines Hoh *et al.* (2021). The r-squared and p-value of the population are shown in the left upper corners of each plot. The progeny are colored as grey dots and the parental lines CB27 and 24-125B-1 indicated by red and blue respectively.

Association of lipid classes and fatty acid profiles with genetic markers.

Relative abundances of lipid classes

Figure S9 and Table S1 describe genetic associations (LOD scores) for relative abundances of classes of lipids and DGDG/MGDG ratio. Multiple lipid classes and the ratio of DGDG/MGDG showed significant associations with genetic markers (QTL intervals) at low temperatures including MGDG (intervals on chromosomes (Chrs) 3 and 4), DGDG (Chrs 4, 6, 8, 9, 10, 11), PG (Chr 11), PEPI (Chr 3), DGDG/MGDG ratio (Chrs 3, 4, 8, 9, 11) (Figures S9A-C and F-G). By contrast, no significant QTL intervals were found for PC or SQDG (Figure S9D-E).

Relative fatty acid compositions

Figure S10 describes genetic associations for FA contents. Several FA groups such as MGDG 16:0, MGDG 18:3, DGDG 18:3, PG 18:3 did not show statistically significant correlations (Figure S10A, C, F and H). By contrast, the contents of a limited number of specific fatty acids showed strong associations to several genomic loci (Figure S10I-M

and O-Q). Figure 3 plots genomic associations for selected fatty acid contents, PG 16:0, PG 18:0, PG 16:1t and PEPI 18:1 with genetic markers across the RIL population. Several distinct patterns of associations were observed. The strongest QTL intervals were observed for PG 16:1t on Chrs 4 and 9 (Figure 3A), with significant genomic associations for PEPI 18:1 on Chrs 4, 7 and 9 (Figure 3B), PG 18:0 on Chrs 3 and 7 (Figure 3C) and PG 16:0 on Chr 7 (Figure 3D).

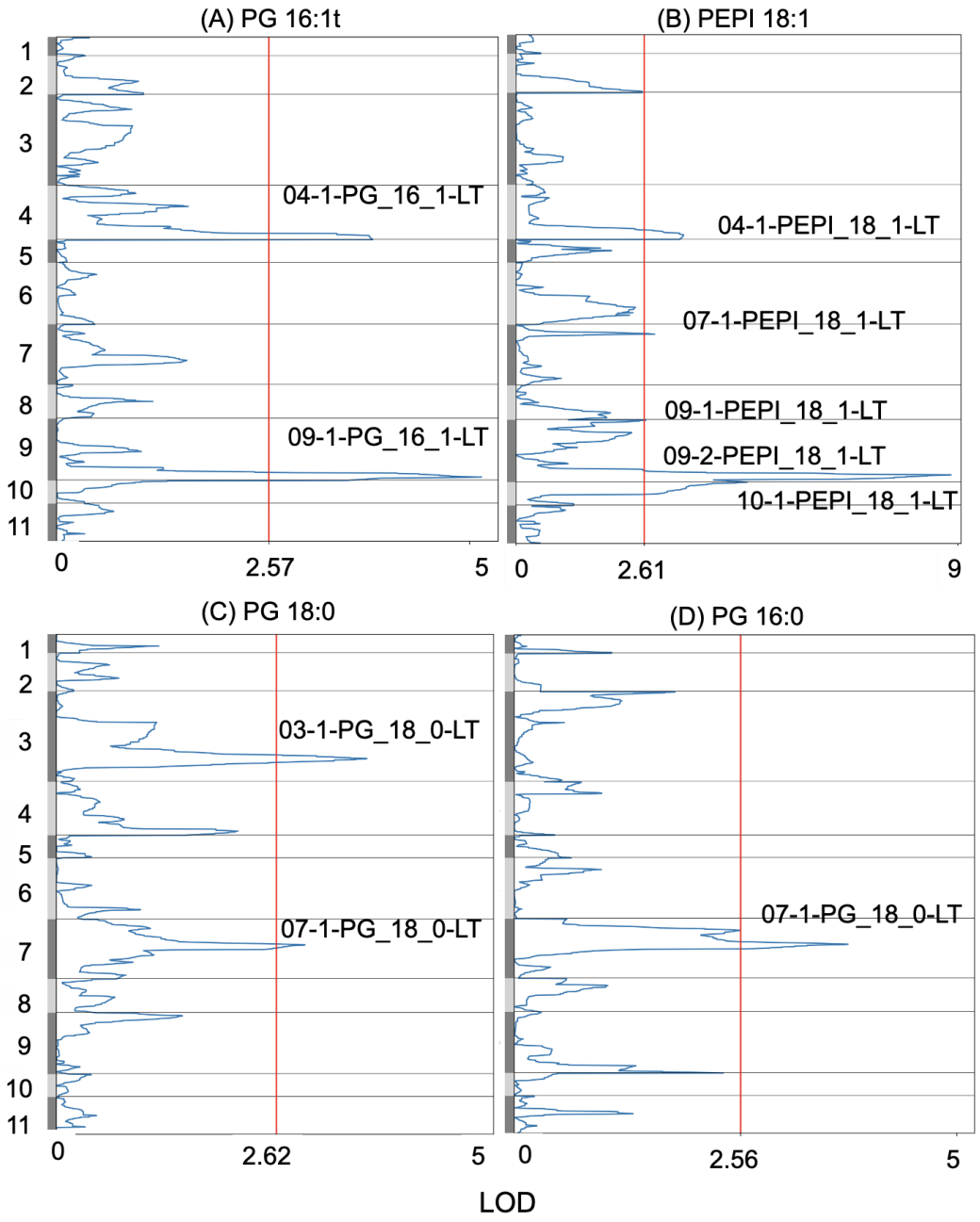

Figure 3. QTL analysis of the contents of selected fatty acids in the chilling condition. Logarithm of odds (LOD) score plots of the contents of selected fatty acids (A, PG 16:1t; B, PEPI 18:1; C, PG 18:0; D, PG 16:0) in the chilling condition measured on the third day of LT. The genetic position is indicated by the y-axis. Significance threshold of 0.05 for each parameter based on 1000 permutations is indicated by the red vertical line. Each QTL named chromosome- index- phenotypes- temperature condition (low temperature, LT) is shown either on the left or right side of the panel with arrows.

Potential co-linkages among photosynthetic parameters and lipid composition.

Co-localization of QTL regions can suggest potential genetic and mechanistic linkages between the processes being probed. We observed such overlaps for QTLs associated with a network of photosynthetic parameters (Φ_{II}, photosynthetic efficiency; qIt, photoinhibition; qL, state of Q_A oxidation) measured in Hoh *et al.* (2021) and the FAs, PG 16:0, PG 18:0, PG 16:1t, HMP-PG, and PEPI 18:1. These observations are summarized as "daisy graphs" (Figure 4) which describe potential associations to common genetic loci. Specific QTL intervals are indicated in the center circles, different phenotypes are indicated by surrounding circles, and the widths of the connecting lines indicate the LOD score for association. Solid and dashed lines indicate linkages above or below our statistical threshold. The color of the connecting lines indicates the "directionality" of the association, with between the phenotype and the allele present in the tolerant (CB27, orange) and sensitive (24-125B-1, blue) lines. For instance, an orange line would indicate a positive association between the presence of the CB27 allele and the measured phenotype. This also indicates a negative association between the presence of the 24-125B-1 allele and the measured phenotype.

Figure 4 shows associations with photosynthetic measurements taken at 1.5 hours prior to the end of Day 3 (Hoh *et al.* 2021). We chose this time because it gave a good representation of a range of LT effects, but similar conclusions can be drawn from other time points. We found significant co-linkages of a range of photosynthetic parameters to

specific QTL intervals on Chrs 4 and 9 at these times, as also discussed in Hoh *et al.* (2021). We also observed strong QTLs for specific FA-lipid class combinations on Chrs 4 (marker positions 50.04-64.45cM), and Chr 9 (marker positions 86.93-104.15cM), which clearly overlap those seen for the photosynthesis parameters, as well as an interval on Chr 7 (marker positions 31-40cM), which did not show apparent overlaps. These overlaps in Chr 4 and Chr 9 suggest possible co-association of the phenotypes with genetic loci in these regions, though as discussed below, we cannot rule out the contributions from multiple loci within these intervals.

The presence of the CB27 alleles in the Chr 4 interval was negatively associated with Φ_{II}, the redox state of Q_A, estimated by the qL parameter, and PEPI 18:1, positively associated with qIt and PG 16:1t. PG 16:0, PG 18:0 and HMP-PG showed no significant associations with other parameters in Chr 4 (Figure 4A). Strikingly, the Chr 9 region showed the inverse relationships, i.e., positive associations with the CB27 alleles for one set of parameters (Φ_{II}, qL, PEPI 18:1) and negative associations for qIt and PG 16:1t. Similar to Chr 4, PG 16:0, PG 18:0 and HMP-PG showed no measurable associations with other parameters in Chr 9 (Figure 4B). On Chr 7, only PG 16:0, PG 18:0 and HMP-PG showed QTL intervals in Chr 7 but these did not overlap those for photosynthetic parameters (Figure 4C), arguing against models where variations in HMP-PG confer altered photosynthetic responses to chilling. These results suggest that the loci on Chrs 4 and 9 have opposing effects on photosynthetic responses which are likely linked to PG 16:1t and/or PEPI 18:1. Interestingly, RILs with combinations of the

two parent genotypes at these locations show more extreme behaviors (see below).

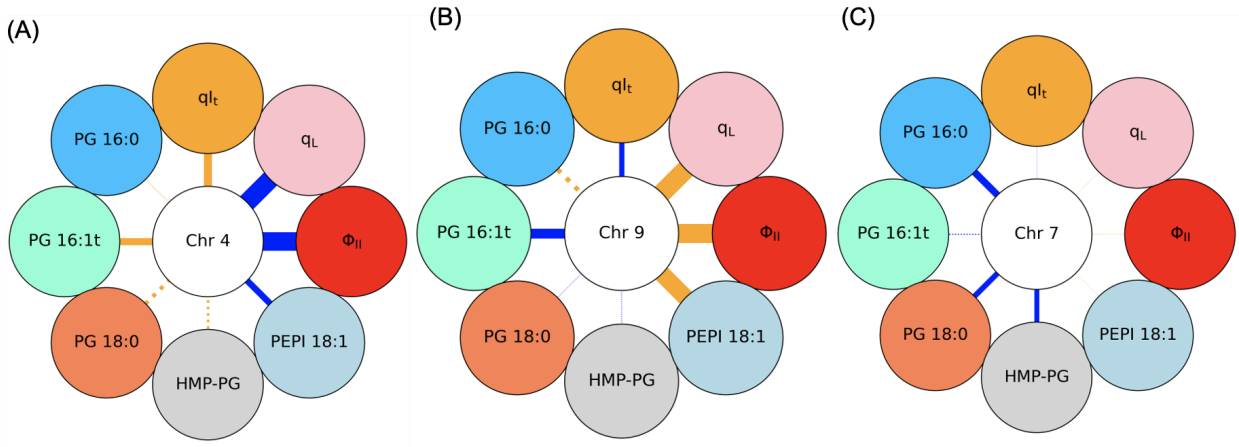

Figure 4. The associations for selected QTL intervals of photosynthetic parameters from DEPI and selected fatty acids in LT at Chr 4, 59.04-64.45 cM (A) and Chr 9, 86.93-104.15 cM (B), Chr 7, 31- 40 cM (C).
LOD score plots from the previous paper (*c.f.* Figure 6 in Hoh *et al.* 2021) were replotted in the form of "daisy graphs," in which a specific Chr is indicated in the center circles, different phenotypes are indicated by surrounding circles, with the thickness of the connecting lines set proportional to the LOD score for association. For more clear visualization, the maximum line width was set at LOD = 10, i.e., scores above 10 were set to this thickness. Solid lines represent significant positive associations between the phenotype and the allele present in the tolerant (CB27, orange) and sensitive (24-125B-1, blue) lines. No significant association of the phenotype (where the LOD score for each phenotype is below the threshold) with the QTL intervals are indicated by either dashed lines or no line.

Effect size contributions of specific QTL intervals to two fatty acids (FAs).

The QTL intervals in Figures S9 and S10 reflect statistical associations between phenotypes and genetic markers, i.e., they indicate that having one genotype is statistically associated with differences in a parameter, but do not tell us by how much

or even in what direction an effect is. In this section, we quantify the apparent impact of a genotype having a particular set of markers. Individual genotypes in the RIL population are homozygous for markers that come from either of the two parental lines. When discussing a single locus, we designate these by letters “AA,” having the allele from CB27 (tolerant, maternal line), or “BB,” having the allele from 24-125B-1 (sensitive, paternal line). The effect sizes were obtained by splitting the population into two groups (those with AA and BB) and averaging the measured values.

Figure 5 shows the dependencies of markers in the QTL on Chr 4 (59.64 cM) and 9 (86.93 cM) on PG 16:1t (Figure 5A) and PEPI 18:1 (Figure 5B). Genotypes with AA at the QTL on Chr 4 showed higher PG 16:1t content compared to those with BB (Figure 5A). By contrast, the opposite was observed for the QTL on Chr 9, with the AA allele imposing a decrease in PG 16:1t content compared to those with BB. Similar, additive but opposing effects of the two QTL regions were also observed in the photosynthetic parameters (e.g., *c.f.* Figure 6 in Hoh *et al.* 2021), supporting a mechanistic connection between the observed variations in lipids and photosynthetic responses.

To test for additivity or epistasis, we assessed the combined effects of both sets of alleles (Figures 5C and 5D), dividing the population into the four possible genetic combinations, AAAA, AABB, BBAA and BBBB for alleles from each parent for Chr 4 and Chr 9, e.g., the AABB genotype has the CB27 allele on the Chr 4 QTL and that for 24-125B-1 in the QTL on Chr 9. Note that AAAA and BBBB showed no significant

differences for FA compositions (Figure S11), and thus we present averaged AAAA and BBBB for each parameter, only showing three groups in Figure 5 C-D. Interestingly, both FAs in AAAA and BBBB genotypes showed similar compositions, whereas AABB genotypes showed the highest for PG 16:1t and lowest for PEPI 18:1 and BBAA showed the opposite. This result parallels those seen for the photosynthetic parameters (*c.f.* Figure 6 in Hoh *et al.* 2021). It also explains, in part, the observed transgressive FA and photosynthetic phenotypes across the RIL population, i.e., more extreme phenotypes were seen in progeny that contain the AABB and BBAA markers.

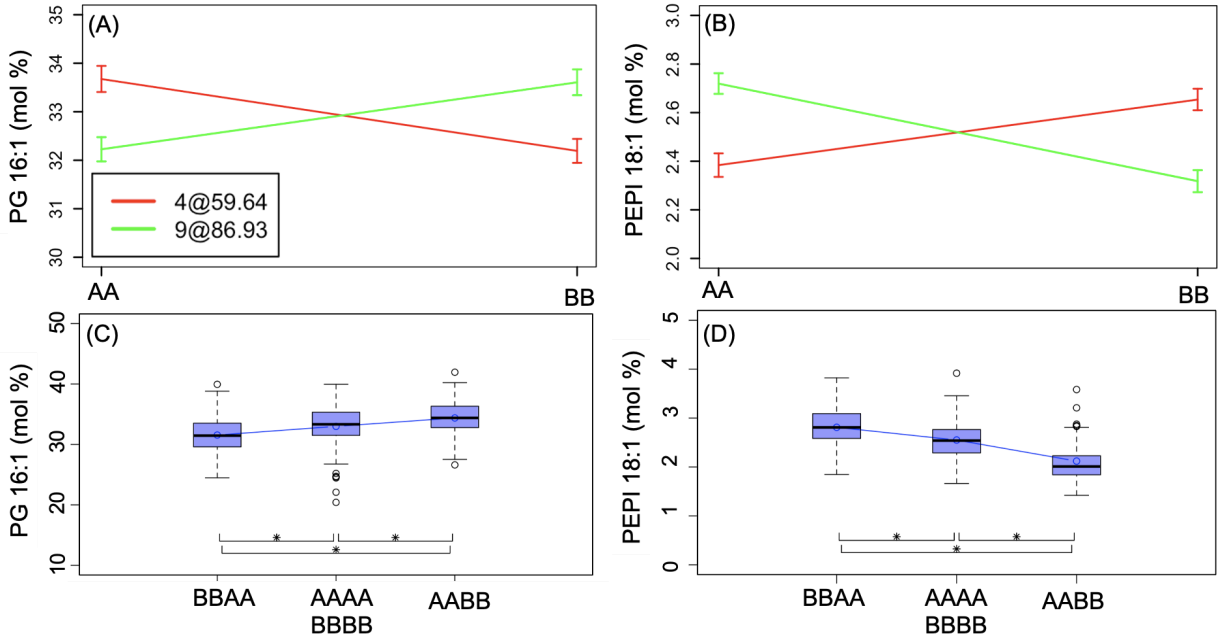

Figure 5. Effect plots for identified QTLs in Chrs 4 and 9 for fatty acid compositions. Panels A and B show mean fatty acid compositions (A, PG 16:1t; B, PEPI 18:1) as dependent on allele for the major QTL intervals on Chr 4, 59.64 cM (red) and Chr 9, 86.93 cM (green). AA and BB represent genotypes with markers for CB27 and 24-125B-1, respectively. Panels C and D show the allelic contributions to fatty acid compositions from combinations from both QTL intervals, where the first two letters represent markers for Chr 4 and the second two letters for Chr 9. See more details in text. The asterisks show significant differences between the genotype groups (as shown in brackets) by t-test ($p<0.05$).

Linkages between Q_A redox states modulating the genetic effects on temperature stress.

To explore possible mechanisms for the FAs and photosynthetic responses, we compared genotype dependencies of more detailed photosynthetic parameters taken from Hoh *et al.* (2021) across the entire RIL population. Figure 6A and B shows average values of qL and qIt against Φ_{II} respectively at 1.5 h prior to the end of Day 3 (206 µmol, m^{-2}, s^{-1}) on Day 3, grouped by their genotypes for QTL on Chr 4 and 9, i.e., those with AAAA, AABB, BBAA and BBBB, as in Figure 5.

Genotypes having the BBAA and AABB genotypes showed the highest and lowest qL on Φ_{II} values ($p<0.05$ by t- test), while those with AAAA and BBBB showed intermediate values (NS) (Figure 6A and Figure S12). The BBAA and AABB genotypes showed the most extreme differences, with the former having lower qIt ($p<0.05$ by t-test) and higher Φ_{II} values ($p<0.05$ by t- test) (Figure S12). These results are consistent with a model (Huner, Öquist & Sarhan 1998) where increased PSII excitation pressure or accumulation of reduced Q_A^-, estimated here by the qL parameter, caused increased rates of PSII photodamage at LT, measured by the qIt parameter. These effects were stronger in the genotypes containing the AABB alleles, which also had the highest PG 16:1t and lowest PEPI 18:1. The opposite was seen for genotypes containing BBAA.

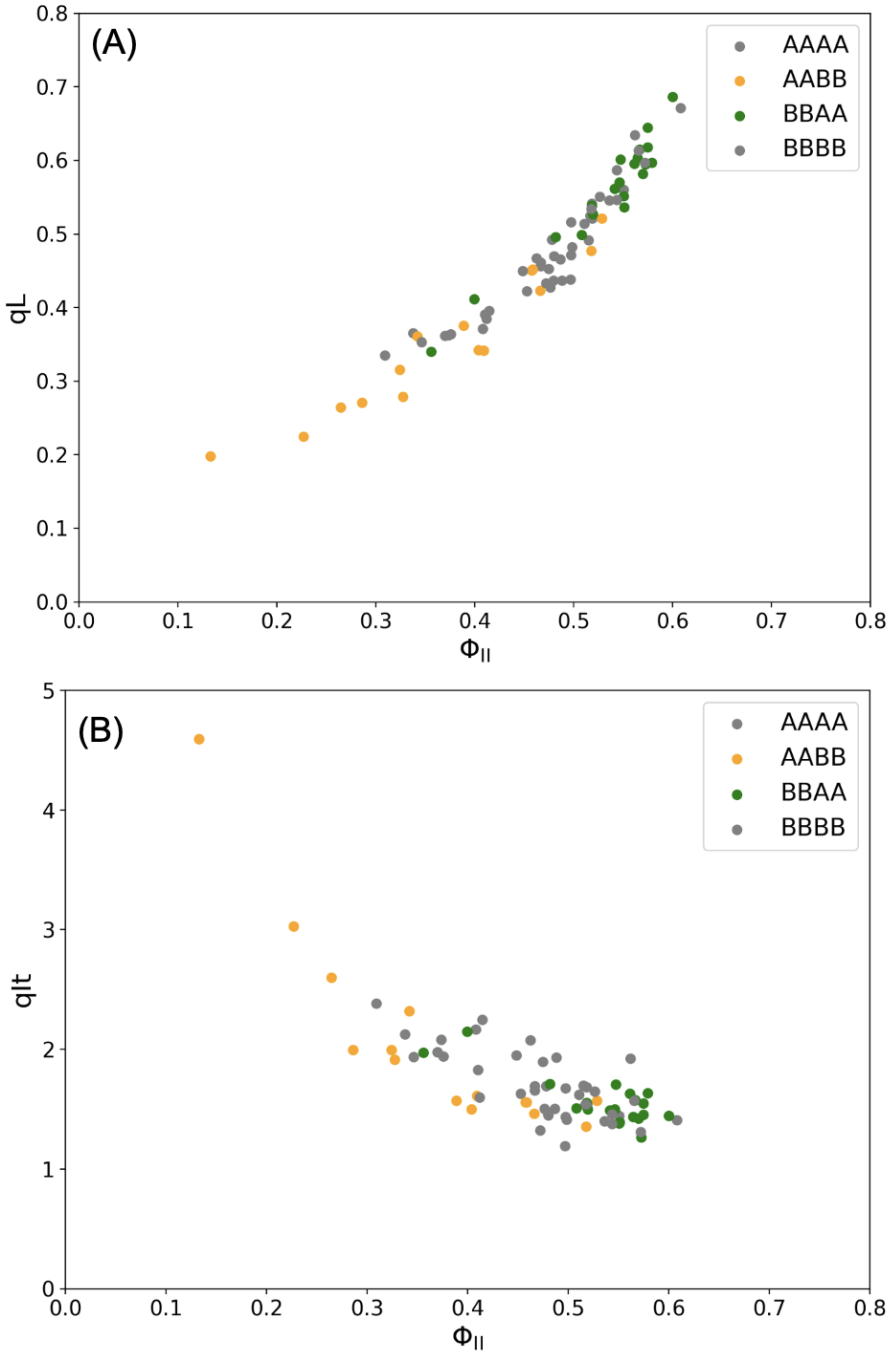

Figure 6. Relationships between photosynthetic responses grouped by different combinations of alleles for the identified QTLs in Chrs 4 and 9 (data is from Hoh *et al.* 2021) (A) qL and (B) qIt against Φ_{II} from DEPI data, at 1.5 h prior to the end of Day 3 (206 µmol, m^{-2}, s^{-1}). The allele groups of AAAA, BBBB are indicated by gray dots. The allele groups of AABB and BBAA are colored orange and green, respectively.

Detailed statistical analyses testing for differences in phenotypes between the allele groups are given in Figure S12.

Altering PG 16:1t composition in Arabidopsis recapitulates the low temperature effects seen in cowpea.

The above quantitative genomics results on the cowpea RIL population are consistent with a linkage between PG 16:1t composition, Q_A redox state and photodamage. If these represent mechanistic (causative) linkages, they could operate in two distinct modes: 1) PG 16:1t abundance may impact photosynthesis, resulting in modulation of photodamage; or 2) photosynthesis may impact PG 16:1t abundance, e.g., photodamage initiates changes in FA composition. To test these possibilities, we assessed the chilling responses of photosynthesis in Arabidopsis lines with modified PG 16:1t abundance, including two FAD4 knockout (KO) mutants (Alonso *et al.* 2003; Gao *et al.* 2009), a FAD4 overproducing (OX) line, which was generated as described in Materials and Methods (Horn et al. 2020), and appropriate wild types (WT), and determined that the knockout lines lacked 16:1t (with corresponding increases in 16:0 PG precursor) whereas the overexpression line showed a ~34% increase in 16:1t (with corresponding decreases in 16:0 PG precursor) compared to WT.

Photosynthesis responses were measured using the fluorescence imaging DEPI chamber under the light regime as used in Figure S1. Because Arabidopsis is more

tolerant of LT, we used 21ºC and 6ºC as the CT and LT conditions.

The photosynthetic responses of *Arabidopsis* WT and mutant lines over a five-day experiment are shown in Figure 7. Day 1 of the experiment was performed at 21°C, named “Arabidopsis Control Temperature” (ACT) to distinguish it from the control experiment used for cowpea. Days 2-5 were performed at 6°C, i.e., “Arabidopsis Low Temperature” (ALT). As described in Cruz *et al.* (Cruz *et al.* 2016), values are presented as heat maps, comparing mutants with Col-0 at each time point. For Φ_{II} and qL, differences were calculated as log fold changes; for NPQ, qE and qI the direct differences were calculated. The lower panel in Figure 7 shows Z-scores for these differences, values beyond the range of -1 to +1 indicate significant differences and are indicated by blue and red coloration.

Under ACT, only small differences were seen in photosynthetic parameters between Col-0 and the mutant lines. Small increases in qE and qL were seen in the *fad4* lines, but these were marginally significant. Larger differences emerged under ALT, consistent with previous work showing that stronger phenotypes tend to emerge under more stressful environmental conditions (Cruz *et al.* 2016).

Under these conditions, *fad4*, which is deficient in PG 16:1t, showed higher Φ_{II} and qL and lower NPQ, qE, qI compared to WT. On the other hand, the *FAD4*-OX line, which has more PG 16:1t compared to WT, showed the opposite effects, with lower Φ_{II} and qL,

higher NPQ, qE, qI. The results are qualitatively similar to those obtained with the chilling sensitive and tolerant genotypes of cowpea, i.e., genotypes with higher levels of PG 16:1t tending to be more sensitive to chilling, with lower Φ_{II} and qL, and higher NPQ and qI (Hoh *et al.* 2021). This result suggests that the abundance of PG 16:1t correlates with similar effects in both species, regardless of whether the species is chilling sensitive. Furthermore, changes in the abundance of this lipid correspond to altered photosynthetic responses at LT.

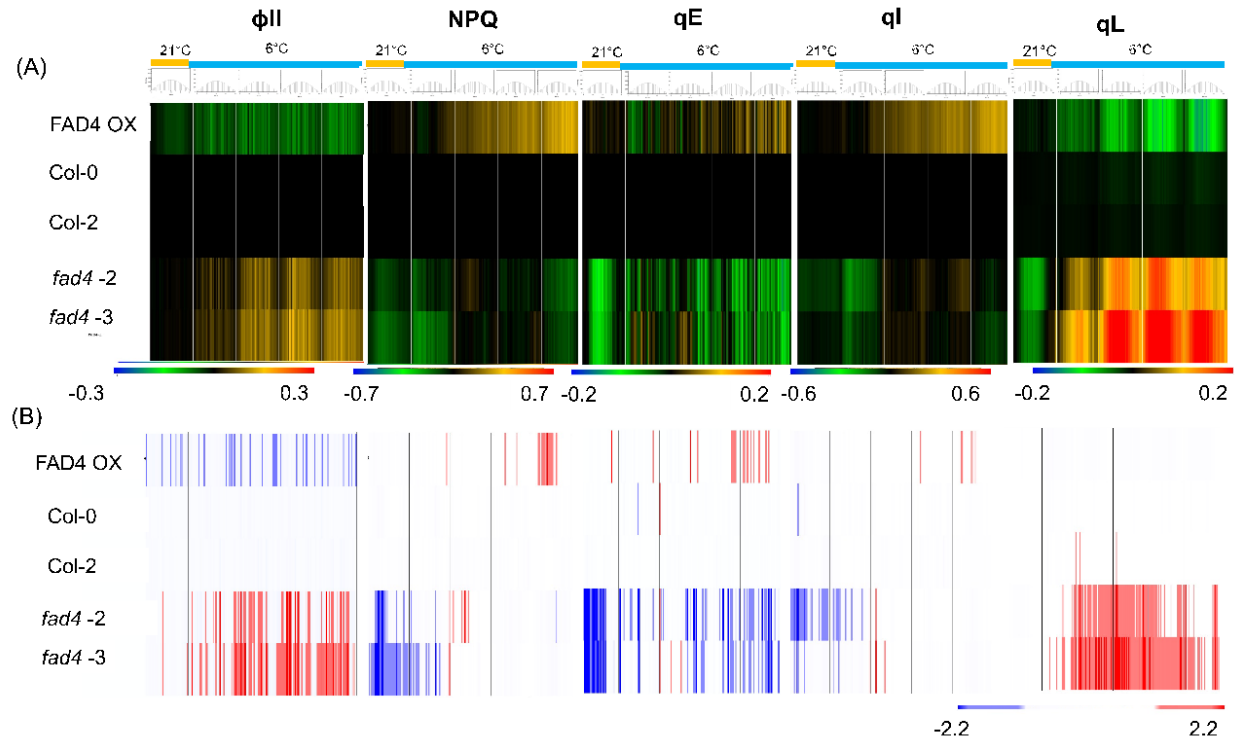

Figure 7. Photosynthetic responses of *Arabidopsis fad4* and FAD4 OX mutants varying PG 16:1t composition. (A) Photosynthesis measurements (Φ_{II}, NPQ, qE, qI and qL) from DEPI chamber under chilling, sinusoidal light conditions. Φ_{II} and qL are presented as log fold changes compared to WT, whereas NPQ, qE, qI are presented as the straight differences with WT (n ≥ 4). *FAD4* -OX line showed lower Φ_{II} and qL while KO line showed higher Φ_{II} and qL. *FAD4*-OX line showed higher qE, qI compared to WT whereas KO lines showed lower qE and qI compared to WT. (B) Z-Scores for differences in photosynthesis parameters between mutant and WT.

DGDG/MGDG ratio for the chilling photosynthetic tolerance

After LT treatment, we observed increases in the DGDG/MGDG ratio in the tolerant line (CB27) after chilling stress (Figure S3), but no significant changes in 24-125B-1. When measured over the RIL population, the DGDG/MGDG ratio showed a QTL interval on Chr 9, which overlapped with that of the photosynthetic parameters under LT (Figure 8B), but not with the QTL on Chr 4. These results suggest a partial co-linkage of the DGDG/MGDG ratio with PG 16:1t and subsequent photosynthetic responses, as indicated in the Daisy plots in Figure 8. The DGDG/MGDG ratio showed higher average values in the tolerant allele group for the QTL on Chr 9 (Figure 8B), consistent with a role in chilling responses.

MGDG is a non-bilayer forming lipid and the DGDG/MGDG ratio affects membrane stability, phase transition, the ability for proteins to insert (Williams 2004; Shimojima & Ohta 2011). It has also been shown that the presence of MGDG in lipid bilayers facilitates the switching of PSII light harvesting complexes from a light-harvesting to energy-quenching modes, possibly to increase photoprotective dissipation of excess light energy (Tietz *et al.* 2020). Chloroplast lipid remodeling under freezing temperatures is catalyzed by SENSITIVE TO FREEZING 2 (SFR2), an enzyme required for freezing tolerance, which acts by transferring galactosyl residues from monogalactolipid to different galactolipid acceptors, forming oligogalactolipids, diacylglycerol and

triacylglycerol, leading to membrane stabilization during freezing conditions (Moellering *et al.* 2010) (Moellering *et al.* 2010). Though *sfr2* has not yet been linked to lipid remodeling under chilling (non-freezing) conditions, such a role would be consistent with our observation of potential linkages between the DGDG/MGDG ratio and photosynthetic responses.

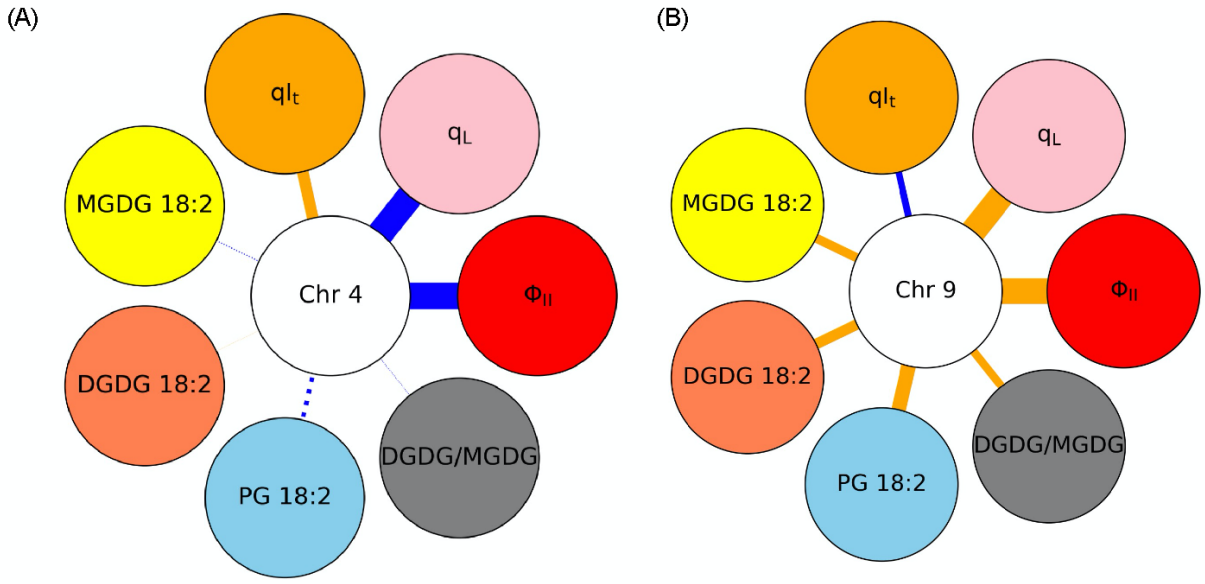

Figure 8. The associations for selected QTL intervals of photosynthetic parameters from DEPI and selected fatty acids in LT at Chr 4, 59.04-64.45 cM (A) and Chr 9, 86.93-104.15 cM (B). LOD score plots from the previous paper (*c.f.* Figure 3 in Hoh *et al.* 2021) were replotted in the form of "Daisy Graphs," in which a specific Chr is indicated in the center circles, and different phenotypes are indicated by surrounding circles, with the thickness of the connecting lines set proportional to the LOD score for association. The maximum line width was set at LOD = 10, and scores above 10 were set to this thickness. Solid lines represent significant positive associations between the phenotype and the allele present in the tolerant (CB27, orange) and sensitive (24-125B-1, blue) lines. Below the threshold each phenotype is shown as dashed lines.

Specific FA and lipid species, rather than bulk unsaturation levels, appear to determine photosynthetic responses to LT.

The lack of significant QTL intervals for FAs 18:3 of MGDG, DGDG, and PG (Figure S10C, F and H) implies that genetic variations in these components are weak or not linked to specific genetic markers, and argues against roles for 18:3 FA species in determining the observed genetic variations in photosynthetic responses in the cowpea RIL population.

Significant QTL intervals did appear for PG 16:0, PG 18:0 and HMP-PG on Chr 7 (Figure 4C) as well as for the 18:2 FAs in MGDG, DGDG, and PG (Figure S10B, E and G) on Chr 9. However, the regions for PG 16:0, PG 18:0 and HMP-PG did not overlap those for photosynthetic parameters, arguing that mappable genetic variations in these components are present in the population, but that these are not linked to mappable variations in photosynthetic responses (Figure 4). The QTL interval for MGDG 18:2, DGDG 18:2, and PG 18:2 on Chr 9 overlapped with those found for photosynthetic parameters (Figure 8B), suggesting potential linkages. Further support for a linkage comes from the positive correlation between these FAs and the presence of alleles from the tolerant line in this interval (Figure 8B). A reasonable interpretation of these results is that MGDG 18:2, DGDG 18:2, and PG 18:2, but not PG 16:0, PG 18:0 and HMP-PG or 18:3 FAs, contribute to photosynthetic chilling tolerance in the cowpea RIL population.

PG 16:1t abundance is functionally linked to photosynthetic responses under chilling conditions.

By analyzing genetic variations in cowpea RILs, we observed co-segregation patterns among photosynthetic parameters, $\Phi_{II,}$ qL, qIt and PG 16:1t and PEPI 18:1, suggesting those FAs are genetically or mechanistically linked with photosynthetic regulation under chilling stress on Chrs 4 and 9 (Figure 4). Higher levels of PG 16:1t and lower levels of PEPI 18:1 are associated with lower photosynthetic efficiency, more reduced Q_A (decreased qL), and increased photoinhibition (qI) at LT (Figure 6). Overall, the results are consistent with models where increased PSII excitation pressure or accumulation of reduced Q_A^-, estimated here by the qL parameter, caused increased rates of PSII photodamage at LT, measured by the qIt parameter (Huner *et al.* 1998) (Huner *et al.* 1998).

PG 16:1t is of particular interest to photosynthesis because it is present in the thylakoid membrane (Selstam 2004), has long been proposed to be important for temperature stress responses (Xu & Siegenthaler 1997), and has been linked to the redox state of the chloroplast (Horn *et al.* 2020). The fact that increased levels of PG 16:1t were associated with decreased tolerance to chilling may be attributable to several possible mechanisms. First, PG 16:1t could have induced sensitivity to cold, e.g., by altering the fluidity of membranes associated with photosynthetic processes. Alternatively, PG 16:1t may accumulate as a result of chilling stress, and thus would be associated with

sensitive genotypes. In Arabidopsis, FAD4 has been shown to require the activity of PRXQ, which uses H_2O_2 as a substrate to oxidize thiol regulated enzymes (Horn *et al.* 2020). For instance, it is possible that chilling stress results in increased H_2O_2 production, leading to activation of PRXQ and accumulation of PG 16:1t. Experiments on a series of *Arabidopsis* lines that either lack (*fad4*) or contain elevated levels (*FAD4*-OX) of FAD4 show that increased levels of PG 16:1t result in decreased photosynthetic efficiency, more reduced Q_A and increased photoinhibition (showing lower Φ_{II} and qL, higher NPQ, qE, qI) at low temperature (Figure 7). Remarkably, decreasing PG 16:1t in cowpea, and eliminating it in the *fad4* mutant, led to increased photosynthetic efficiency and decreased photoinhibition under LT. These results support the former model, where PG 16:1t affects the photosynthetic responses at LT, rather than resulting from the stress (but see also below).

If PG 16:1t does determine LT photosynthetic responses, one may reasonably ask why PG 16:1t would accumulate if it led to decreased performance. One possibility is that PG 16:1t may have a protective (or adaptive) role under different conditions, e.g., at higher temperatures, resulting in the tradeoff of less resilient photosynthesis under LT. In this context, it is noteworthy that cowpea is mainly a warm climate crop and may not be selected for optimal responses to chilling. Another possibility is that PG 16:1t is involved in a signaling pathway that both responds to stress and downregulates photosynthetic responses, as suggested by the involvement of PRXQ and H_2O_2 in its activity (Horn *et al.* 2020). In this scenario, the increased PG 16:1t levels in the cowpea lines could

reflect increased ROS production under LT stress, while manipulating FAD4 in Arabidopsis could reflect a bypassing of the normal regulatory processes, leading to altered effects on photosynthesis.

Candidate genes in PG 16:1t QTL intervals

We found significant co-linkages between photosynthetic parameters and PG 16:1t contents in QTL intervals on Chrs 4 and 9 (Fig. 4). Here we explore possible candidate genes common to the regions linked to both PG 16:1t and photosynthetic phenotypes. As described in Hoh *et al.* (2021), we considered two sets of intervals, the most restrictive regions that were common to all sets of parameters considered, and the most inclusive, i.e., linked to any of the phenotypes considered.

The restrictive region for Chr 9, which spans 93.76 - 95.95cM (flanking markers, 2_11917 and 2_22085), and contains 68 candidate genes (Table S8 in Hoh *et al.* 2021). One intriguing candidate gene in this region is thioredoxin-h1 (trx-h1) (*Vigun09g249200*). The biosynthesis of PG 16:1t is stimulated by PRXQ activity (Horn *et al.* 2020), and trx-h1 could mediate redox interactions between photosynthetic reductants and production of PG 16:1t. It has been reported (Hara & Hisabori 2013) that trx-h1 interacts with PrxQ, suggesting a model where the observed co-linkages were mediated by altered reductant and/or ROS generated by photosynthesis through trx-h1 and PRXQ. This possibility is also suggested by reports that peroxiredoxins (Rouhier *et al.* 2001; Marx, Wong & Buchanan 2003; Maeda, Finnie & Svensson 2004) and

non-specific lipid transfer protein (Maeda *et al.* 2004) are potential target proteins of trx-h1.

In Chr 4, the restrictive region spans between 60 - 60.93 cM (flanking markers, 2_00148 and 2_07328), and contains 79 candidate genes, see Table S6 in Hoh *et al.* 2021. As mentioned in Hoh *et al.* 2021, on candidate gene in this region is Deg1 (*Vigun04g188700*), a protease located in the thylakoid lumen and which has been previously shown to be involved in PSII repair, degrading the D1 (Kapri-Pardes, Naveh & Adam 2007) and OE33 subunits of PSII, as well as plastocyanin (Chassin, Kapri-Pardes, Sinvany, Arad & Adam 2002). It was reported (Kanervo, Aro & Murata 1995; Moon, Higashi, Gombos & Murata 1995) that changes in saturation/unsaturation levels of FAs affect the extent of PSII photoinhibition, consistent with our observation that certain allele combinations within this region modulate the rates of PSII photodamage and repair (Figs. 7,8 and 9 in Hoh *et al.* 2021), and are linked to the contents of PG 16:1t (Figs. 5 and 6). It is thus conceivable that lipid content could impact the role of Deg1, leading to linkage between PG 16:1t and PSII photoinhibition. Another candidate gene in this region is *Vigun04g193600* (homologous to the *Arabidopsis* gene at AT5G14720) identified as a regulator of thermomorphogenesis (Vu *et al.* 2021), with possible connections to chilling responses.

The more inclusive QTL region on Chr 4 spanned 34.47 - 64.45cM (flanking markers, 2_10801 and 2_04962) encompasses a total of 712 predicted coding regions (Table S7

in Hoh *et al.* 2021). Potential loci in this region include several photosynthesis-related genes such as the light-harvesting complex of photosystem II (LHCII) 5 (*Vigun04g167600*) and ferredoxin thioredoxin reductase (FTR) (*Vigun04g181000*). These have potential connections to redox regulation and ROS production (Horn 2021).

Another candidate gene in the inclusive Chr 4 region, *Vigun04g201600,* is homologous to AT3G18280 in *Arabidopsis*, which is reported to be involved in lipid binding and transport, and undergoes expression level changes in response to changes in temperature (Swindell, Huebner & Weber 2007). While we do not expect such lipid transporters to directly impact PG 16:1t levels, there could be global effects on lipid compositions that result in compensatory changes in PG 16:1t.

The more inclusive region on Chr 9 QTL spanned 56.08-104.15cM (flanking markers, 2_01496 and 2_23951), and encompassed 1242 predicted coding regions (Table S9 in Hoh *et al.* 2021). This region contained additional members of the thioredoxin superfamily (*Vigun09g154700, Vigun09g167600, Vigun09g224600, Vigun09g238200 and Vigun09g256300*), thioredoxin M-type 4 (*Vigun09g156800*) and several photosynthesis-related genes including the petM subunit of the cytochrome b6f (*Vigun09g241500*), photosystem II subunit X (*Vigun09g221400*), Mog1/PsbP/DUF1795-like photosystem II reaction center PsbP family protein (*Vigun09g156000 and Vigun09g204000*), photosystem II 22kDa protein (psbS) (*Vigun09g165900*), plastocyanin (petE) (*Vigun09g257300*), the PsbP (PSII reaction

center family protein, *Vigun09g263400*), ATP synthase epsilon chain *(Vigun09g163500*), subunit NDH-M of NAD(P)H:plastoquinone dehydrogenase complex (*Vigun09g160700*), ferredoxin-related (*Vigun09g220600*), and PSI light-harvesting complex gene 5 (*Vigun09g238500*), all of which could, in principle, contribute to chilling responses. It has been suggested that PG is important for PSII structure and function (Jordan, Chow & Baker 1983; Kruse, Radunz & Schmid 1994; Kruse & Schmid 1995) as well as in LHCII trimerization (Duval, Tremolieres & Dubacq 1979; Dubacq & Tremolieres 1983; Krupa 1984; Horváth, Droppa, Hideg, Rózsa & Farkas 1989) and PSII oligomerization (Duval *et al.* 1979), though these effects are probably not specific to PG 16:1t.

Conclusions: Exploring natural variations to identify linkages and their mechanistic bases and implications for improving crop responses to climate change

The results highlight some advantages of using natural genetic variations to identify underlying mechanisms. Because classical genetics approaches introduce (often deleterious) mutations that are not commonly found in natural populations, it can miss variations that have evolved to adapt to specific environments, and thus may be important for improving crop responses to changing environmental conditions.
The current work identified several QTL intervals for photosynthetic and lipid compositional responses to chilling. In principle, these loci can be immediately used in

breeding efforts to address a key limitation to cowpea cultivation. One interesting observation is that the parent lines containing two major QTL, on Chrs 4 and 9, appear to operate with opposing effects on both FA composition (Figures 4 and 5) and photosynthetic responses to chilling (Hoh *et al.* 2021). Thus, the RIL population, containing allelic combinations of these two loci, show more extreme (transgressive) responses than the parents, and may reflect tradeoffs that impact performance under a range of environmental conditions.

The observed linkages, between photosynthetic parameters and lipid composition, showed the important roles of lipids in chloroplasts responding to adverse environmental conditions, and identified potential mechanistic bases for these variations. The most important finding was to identify strong linkages to specific chloroplast lipid molecular species, rather than the general level of unsaturation. This points to the potential roles of these specific lipid components for maintaining the photosynthetic apparatus or signaling in response to stress. In one particular case, these linkages were substantiated by experiments using genetically modified Arabidopsis, leading to a model where PG 16:1t could affect photosynthetic responses under LT, possibly as a component of a signaling pathway.

Finally, as discussed in Hoh *et al.* (2021), there are several caveats on inferring causation from co-linkages, including the possibilities of multiple traits under QTL intervals (see also above). Some variations can be determined by multiple

polymorphisms with small effects and thus might not be revealed by statistical analyses. These small variations are unlikely to be manipulated by breeding, and thus we focused on those that are highly correlated with variations in markers. Indeed, the role of PG 16:1t has been enigmatic and the apparent inverse correlation of PG 16:1t content and photosynthetic performance independently observed in both plant species is remarkable as it clearly implicates this particular lipid in a mechanism protecting photosynthesis against chilling temperatures. As peroxiredoxin PRXQ is required for the efficient synthesis of PG 16:1t (Horn *et al.* 2020), this lipid species may be part of a signaling process that senses the redox state of the chloroplast, which is affected by the performance of the photosynthetic electron transport chain in response to stress. How a reduced level of PG 16:1t can mitigate the negative effects of chilling on photosynthetic efficiency, remains to be explored.

Author contributions

Donghee Hoh (DH), CB and DMK conceived of the experiments. DH and David Hall planned and conducted experiments. DH, AK, PH, CB, JF, JC and DMK interpreted data. All authors contributed to data analyses and interpretation, data mining, writing and revision of the manuscript. All authors approve of the final manuscript.

Acknowledgments

The authors thank Mark Aarts, Padraic Flood, Jeremy Harbinson (Wageningen university) Wellington Muchero (Oak Ridge National Laboratory), Philip A. Roberts, Bao-Lam Huynh, Tim Close (UC Riverside), Christopher Oakley (Purdue University) and

Doug Schemske (MSU) for helpful discussion on QTL analysis, Mike Thomashow (MSU) for discussion on chilling effects and John Browse (Washington State University) for discussion on membrane lipids.

The high throughput phenotyping, lipid profiling and generation and characterization of Arabidopsis mutants were supported by the DOE Office of Science, Basic Energy Sciences under Award DE- FG02-91ER20021 and the MSU Center for Advanced Algal and Plant Phenotyping (CAAPP). Detailed photosynthetic measurements on both cowpea and Arabidopsis lines were supported by the U.S. Department of Energy (DOE), Office of Science, Basic Energy Sciences (BES) under Award no. DE-SC0007101. DH was partially supported by a MSU Plant Science Fellowship. DMK and CB were partially supported by MSU AgBioResearch program.

Bibliography

Alonso J.M., Stepanova A.N., Leisse T.J., Kim C.J., Chen H., Shinn P., … Ecker J.R. (2003) Genome-wide insertional mutagenesis of *Arabidopsis thaliana*. *Science* 301, 653–657.

Anderson J.M. (1986) Photoregulation of the composition, function, and structure of thylakoid membranes. *Annual Review of Plant Physiology* 37, 93–136.

Aronsson H., Schöttler M.A., Kelly A.A., Sundqvist C., Dörmann P., Karim S. & Jarvis P. (2008) Monogalactosyldiacylglycerol deficiency in Arabidopsis affects pigment composition in the prolamellar body and impairs thylakoid membrane energization and photoprotection in leaves. *Plant Physiology* 148, 580–592.

Babiychuk E., Müller F., Eubel H., Braun H.-P., Frentzen M. & Kushnir S. (2003) Arabidopsis phosphatidylglycerophosphate synthase 1 is essential for chloroplast differentiation, but is dispensable for mitochondrial function. *The Plant Journal: for Cell and Molecular Biology* 33, 899–909.

Barkan L., Vijayan P., Carlsson A.S., Mekhedov S. & Browse J. (2006) A suppressor of fab1 challenges hypotheses on the role of thylakoid unsaturation in photosynthetic function. *Plant Physiology* 141, 1012–1020.

Broman K.W. & Sen S. (2009) *A Guide to QTL Mapping with R/qtl*. Springer New York, New York, NY.

Chassin Y., Kapri-Pardes E., Sinvany G., Arad T. & Adam Z. (2002) Expression and characterization of the thylakoid lumen protease DegP1 from Arabidopsis. *Plant Physiology* 130, 857–864.

Cook R., Lupette J. & Benning C. (2021) The role of chloroplast membrane lipid metabolism in plant environmental responses. *Cells* 10.

Cruz J.A., Savage L.J., Zegarac R., Hall C.C., Satoh-Cruz M., Davis G.A., … Kramer D.M. (2016) Dynamic environmental photosynthetic imaging reveals emergent phenotypes. *Cell Systems* 2, 365–377.

Curtis M.D. & Grossniklaus U. (2003) A gateway cloning vector set for high-throughput functional analysis of genes in planta. *Plant Physiology* 133, 462–469.

Dörmann P., Hoffmann-Benning S., Balbo I. & Benning C. (1995) Isolation and characterization of an Arabidopsis mutant deficient in the thylakoid lipid digalactosyl diacylglycerol. *The Plant Cell* 7, 1801–1810.

Dubacq J.P. & Tremolieres A. (1983) Occurrence and function of phosphatidylglycerol containing delta 3-trans-hexadecenoic acid in photosynthetic lamellae. *Physiologie végétale*.

Duval J.C., Tremolieres A. & Dubacq J.P. (1979) The possible role of transhexadecenoic acid and phosphatidylglycerol in light reactions of photosynthesis: the photochemistry and fluorescence properties of young pea leaf chloroplasts treated by phospholipase A2. *FEBS letters* 106, 414–418.

Fujii S., Kobayashi K., Nakamura Y. & Wada H. (2014) Inducible knockdown of MONOGALACTOSYLDIACYLGLYCEROL SYNTHASE1 reveals roles of galactolipids in organelle differentiation in Arabidopsis cotyledons. *Plant Physiology* 166, 1436–1449.

Gao J., Ajjawi I., Manoli A., Sawin A., Xu C., Froehlich J.E., … Benning C. (2009) FATTY ACID DESATURASE4 of Arabidopsis encodes a protein distinct from characterized fatty acid desaturases. *The Plant Journal: for Cell and Molecular Biology* 60, 832–839.

Guo J., Zhang Z., Bi Y., Yang W., Xu Y. & Zhang L. (2005) Decreased stability of photosystem I in dgd1 mutant of Arabidopsis thaliana. *FEBS Letters* 579, 3619–3624.

Hagio M., Sakurai I., Sato S., Kato T., Tabata S. & Wada H. (2002) Phosphatidylglycerol is essential for the development of thylakoid membranes in Arabidopsis thaliana. *Plant & Cell Physiology* 43, 1456–1464.

Hara S. & Hisabori T. (2013) Kinetic analysis of the interactions between plant thioredoxin and target proteins. *Frontiers in plant science* 4, 508.

Härtel H., Lokstein H., Dörmann P., Grimm B. & Benning C. (1997) Changes in the composition of the photosynthetic apparatus in the galactolipid-deficient dgd1 mutant of Arabidopsis thaliana. *Plant Physiology* 115, 1175–1184.

Himelblau E., Mira H., Lin S.J., Culotta V.C., Peñarrubia L. & Amasino R.M. (1998) Identification of a functional homolog of the yeast copper homeostasis gene ATX1 from Arabidopsis. *Plant Physiology* 117, 1227–1234.

Hoh D., Osei-Bonsu I., Chattopadhyay A., Kanazawa A., Fisher N., Tessmer O., … Kramer D.M. (2021) Genetic variation in photosynthetic responses to chilling modulates proton motive force, cyclic electron flow and photosystem II photoinhibition. *Authorea, Inc.* October 14, 2021. DOI: 10.22541/au.163422290.08126533/v1

Horn P.J. (2021) Where do the electrons go? How numerous redox processes drive phytochemical diversity. *Phytochemistry reviews : proceedings of the Phytochemical Society of Europe* **20**, 367–407.

Hölzl G., Witt S., Gaude N., Melzer M., Schöttler M.A. & Dörmann P. (2009) The role of diglycosyl lipids in photosynthesis and membrane lipid homeostasis in Arabidopsis. *Plant Physiology* 150, 1147–1159.

Hölzl G., Witt S., Kelly A.A., Zähringer U., Warnecke D., Dörmann P. & Heinz E. (2006) Functional differences between galactolipids and glucolipids revealed in photosynthesis of higher plants. *Proceedings of the National Academy of Sciences of the United States of America* 103, 7512–7517.

Horn P.J., Smith M.D., Clark T.R., Froehlich J.E. & Benning C. (2020) PEROXIREDOXIN Q stimulates the activity of the chloroplast 16:1Δ3trans FATTY ACID DESATURASE4. *The Plant Journal: for Cell and Molecular Biology* 102, 718–729.

Horváth G., Droppa M., Hideg É., Rózsa Z. & Farkas T. (1989) The role of phospholipids in regulating photosynthetic electron transport activities: treatment of chloroplasts with phospholipase A2. *Journal of Photochemistry and Photobiology B: Biology* 3, 515–527.

Hugly S. & Somerville C. (1992) A role for membrane lipid polyunsaturation in chloroplast biogenesis at low temperature. *Plant Physiology* 99, 197–202.

Huner N.P.A., Öquist G. & Sarhan F. (1998) Energy balance and acclimation to light and cold. *Trends in Plant Science* 3, 224–230.

Hurlock A.K., Roston R.L., Wang K. & Benning C. (2014) Lipid trafficking in plant cells. *Traffic* 15, 915–932.

Huynh B.-L., Ehlers J.D., Huang B.E., Muñoz-Amatriaín M., Lonardi S., Santos J.R.P., … Roberts P.A. (2018) A multi-parent advanced generation inter-cross (MAGIC) population for genetic analysis and improvement of cowpea (Vigna unguiculata L. Walp.). *The Plant Journal: for Cell and Molecular Biology* 93, 1129–1142.

Ivanov A.G., Hendrickson L., Krol M., Selstam E., Oquist G., Hurry V. & Huner N.P.A. (2006) Digalactosyl-diacylglycerol deficiency impairs the capacity for photosynthetic intersystem electron transport and state transitions in Arabidopsis thaliana due to

photosystem I acceptor-side limitations. *Plant & Cell Physiology* 47, 1146–1157.
Jordan B.R., Chow W.-S. & Baker A.J. (1983) The role of phospholipids in the molecular organisation of pea chloroplast membranes. Effect of phospholipid depletion on photosynthetic activities. *Biochimica et Biophysica Acta (BBA)-Bioenergetics* 725, 77–86.
Kanervo E., Aro E.M. & Murata N. (1995) Low unsaturation level of thylakoid membrane lipids limits turnover of the D1 protein of photosystem II at high irradiance. *FEBS Letters* 364, 239–242.
Kapri-Pardes E., Naveh L. & Adam Z. (2007) The thylakoid lumen protease Deg1 is involved in the repair of photosystem II from photoinhibition in Arabidopsis. *The Plant Cell* 19, 1039–1047.
Kobayashi K., Kondo M., Fukuda H., Nishimura M. & Ohta H. (2007) Galactolipid synthesis in chloroplast inner envelope is essential for proper thylakoid biogenesis, photosynthesis, and embryogenesis. *Proceedings of the National Academy of Sciences of the United States of America* 104, 17216–17221.
Kobayashi K., Narise T., Sonoike K., Hashimoto H., Sato N., Kondo M., … Ohta H. (2013) Role of galactolipid biosynthesis in coordinated development of photosynthetic complexes and thylakoid membranes during chloroplast biogenesis in Arabidopsis. *The Plant Journal: for Cell and Molecular Biology* 73, 250–261.
Krupa Z. (1984) The action of lipases on chloroplast membranes. III. The effect of lipid hydrolysis on chlorophyll-protein complexes in thylakoid membranes. *Photosynthesis research* 5, 177–184.
Kruse O., Radunz A. & Schmid G.H. (1994) Phosphatidylglycerol and ß-Carotene Bound onto the D 1-Core Peptide of Photosystem II in the Filamentous Cyanobacterium. *Zeitschrift für Naturforschung C* 49, 115–124.
Kruse O. & Schmid G.H. (1995) The role of phosphatidylglycerol as a functional effector and membrane anchor of the D1-core peptide from photosystem II-particles of the cyanobacterium Oscillatoria chalybea. *Zeitschrift für Naturforschung C* 50, 380–390.
Kunst L., Browse J. & Somerville C. (1989) A mutant of Arabidopsis deficient in desaturation of palmitic Acid in leaf lipids. *Plant Physiology* 90, 943–947.
Li-Beisson Y., Shorrosh B., Beisson F., Andersson M.X., Arondel V., Bates P.D., … Ohlrogge J. (2013) Acyl-lipid metabolism. *The Arabidopsis book / American Society of Plant Biologists* 11, e0161.
Lonardi S., Muñoz-Amatriaín M., Liang Q., Shu S., Wanamaker S.I., Lo S., … Close T.J. (2019) The genome of cowpea (Vigna unguiculata [L.] Walp.). *The Plant Journal: for Cell and Molecular Biology* 98, 767–782.
Lyons J.M. (1973) Chilling Injury in Plants. *Annual Review of Plant Physiology* 24, 445–466.
Maeda K., Finnie C. & Svensson B. (2004) Cy5 maleimide labelling for sensitive

detection of free thiols in native protein extracts: identification of seed proteins targeted by barley thioredoxin h isoforms. *The Biochemical Journal* 378, 497–507.
Maksymiec W., Russa R., Urbanik-Sypniewska T. & Baszyński T. (1992) Changes in acyl lipid and fatty acid composition in thylakoids of copper non-tolerant spinach exposed to excess copper. *Journal of Plant Physiology* 140, 52–55.
Marx C., Wong J.H. & Buchanan B.B. (2003) Thioredoxin and germinating barley: targets and protein redox changes. *Planta* 216, 454–460.
Miquel M., James D., Dooner H. & Browse J. (1993) Arabidopsis requires polyunsaturated lipids for low-temperature survival. *Proceedings of the National Academy of Sciences of the United States of America* 90, 6208–6212.
Moellering E.R., Muthan B. & Benning C. (2010) Freezing tolerance in plants requires lipid remodeling at the outer chloroplast membrane. *Science* 330, 226–228.
Mongrand S., Bessoule J.-J., Cabantous F. & Cassagne C. (1998) The C16: 3\C18: 3 fatty acid balance in photosynthetic tissues from 468 plant species. *Phytochemistry* 49, 1049–1064.
Moon B.Y., Higashi S., Gombos Z. & Murata N. (1995) Unsaturation of the membrane lipids of chloroplasts stabilizes the photosynthetic machinery against low-temperature photoinhibition in transgenic tobacco plants. *Proceedings of the National Academy of Sciences of the United States of America* 92, 6219–6223.
Muchero W., Diop N.N., Bhat P.R., Fenton R.D., Wanamaker S., Pottorff M., … Close T.J. (2009) A consensus genetic map of cowpea [Vigna unguiculata (L) Walp.] and synteny based on EST-derived SNPs. *Proceedings of the National Academy of Sciences of the United States of America* 106, 18159–18164.
Murata N. & Nishida I. (1990) Lipids in relation to chilling sensitivity of plants. *Chilling injury of horticultural crops*.
Murata N., Sato N., Takahashi N., Hamazaki Y. %J P. & Cell Physiology (1982) Compositions and positional distributions of fatty acids in phospholipids from leaves of chilling-sensitive and chilling-resistant plants. 23, 1071–1079.
Murata N. & Yamaya J. (1984) Temperature-dependent phase behavior of phosphatidylglycerols from chilling-sensitive and chilling-resistant plants. *Plant Physiology* 74, 1016–1024.
Murata N. (1983) Molecular Species Composition of Phosphatidylglycerols from Chilling-Sensitive and Chilling-Resistant Plants. *Plant and Cell Physiology* 24, 81–86.
Pribil M., Labs M. & Leister D. (2014) Structure and dynamics of thylakoids in land plants. *Journal of Experimental Botany* 65, 1955–1972.
Raison J.K. (1973) Temperature-induced phase changes in membrane lipids and their influence on metabolic regulation. pp. 485–512.
Reifarth F., Christen G., Seeliger A.G., Dörmann P., Benning C. & Renger G. (1997)

Modification of the water oxidizing complex in leaves of the dgd1 mutant of Arabidopsis thaliana deficient in the galactolipid digalactosyldiacylglycerol. *Biochemistry* 36, 11769–11776.

Roughan P.G. (1985) Phosphatidylglycerol and chilling sensitivity in plants. *Plant Physiology* 77, 740–746.

Rouhier N., Gelhaye E., Sautiere P.E., Brun A., Laurent P., Tagu D., … Jacquot J.P. (2001) Isolation and characterization of a new peroxiredoxin from poplar sieve tubes that uses either glutaredoxin or thioredoxin as a proton donor. *Plant Physiology* 127, 1299–1309.

Routaboul J.M., Fischer S.F. & Browse J. (2000) Trienoic fatty acids are required to maintain chloroplast function at low temperatures. *Plant Physiology* 124, 1697–1705.

Selstam E. (2004) Development of Thylakoid Membranes with Respect to Lipids. In *Lipids in photosynthesis: structure, function and genetics*. (eds S. Paul-André & M. Norio), pp. 209–224. Kluwer Academic Publishers, Dordrecht.

Shimojima M. & Ohta H. (2011) Critical regulation of galactolipid synthesis controls membrane differentiation and remodeling in distinct plant organs and following environmental changes. *Progress in lipid research* 50, 258–266.

Siegenthaler P.-A. & Murata N. (2006) Lipids in Photosynthesis: An Overview. In *Lipids in photosynthesis: structure, function and genetics*. (eds P.-A. Siegenthaler & N. Murata), pp. 1–20. Springer Science & Business Media.

Steffen R., Kelly A.A., Huyer J., Dörmann P. & Renger G. (2005) Investigations on the reaction pattern of photosystem II in leaves from Arabidopsis thaliana wild type plants and mutants with genetically modified lipid content. *Biochemistry* 44, 3134–3142.

Swindell W.R., Huebner M. & Weber A.P. (2007) Plastic and adaptive gene expression patterns associated with temperature stress in Arabidopsis thaliana. *Heredity* 99, 143–150.

Tietz S., Leuenberger M., Höhner R., Olson A.H., Fleming G.R. & Kirchhoff H. (2020) A proteoliposome-based system reveals how lipids control photosynthetic light harvesting. *The Journal of Biological Chemistry* 295, 1857–1866.

Vu L.D., Xu X., Zhu T., Pan L., van Zanten M., de Jong D., … De Smet I. (2021) The membrane-localized protein kinase MAP4K4/TOT3 regulates thermomorphogenesis. *Nature Communications* 12, 2842.

Wang Z. & Benning C. (2011) Arabidopsis thaliana polar glycerolipid profiling by thin layer chromatography (TLC) coupled with gas-liquid chromatography (GLC). *Journal of visualized experiments: JoVE*.

Williams W.P. (2004) The physical properties of thylakoid membrane lipids and their relation to photosynthesis. In *Lipids in photosynthesis: structure, function and*

genetics. (eds S. Paul-André & M. Norio), pp. 103–118. Kluwer Academic Publishers, Dordrecht.

Wolter F.P., Schmidt R. & Heinz E. (1992) Chilling sensitivity of Arabidopsis thaliana with genetically engineered membrane lipids. *The EMBO Journal* 11, 4685–4692.

Wu J. & Browse J. (1995) Elevated Levels of High-Melting-Point Phosphatidylglycerols Do Not Induce Chilling Sensitivity in an Arabidopsis Mutant. *The Plant Cell* 7, 17–27.

Wu J., Lightner J. & Warwick N. (1997) Low-temperature damage and subsequent recovery of fab1 mutant Arabidopsis exposed to 2 [deg] C. *Plant Physiology* 113, 347–356.

Wu W., Ping W., Wu H., Li M., Gu D. & Xu Y. (2013) Monogalactosyldiacylglycerol deficiency in tobacco inhibits the cytochrome b6f-mediated intersystem electron transport process and affects the photostability of the photosystem II apparatus. *Biochimica et Biophysica Acta* 1827, 709–722.

Xu C., Härtel H., Wada H., Hagio M., Yu B., Eakin C. & Benning C. (2002) The pgp1 mutant locus of Arabidopsis encodes a phosphatidylglycerolphosphate synthase with impaired activity. *Plant Physiology* 129, 594–604.

Xu Y. & Siegenthaler P.A. (1997) Low Temperature Treatments Induce an Increase in the Relative Content of Both Linolenic and 3-Hexadecenoic Acids in Thylakoid Membrane Phosphatidylglycerol of Squash Cotyledons. *Plant and Cell Physiology* 38, 611–618.

Yu B. & Benning C. (2003) Anionic lipids are required for chloroplast structure and function in Arabidopsis. *The Plant Journal: for Cell and Molecular Biology* 36, 762–770.

Yu L., Zhou C., Fan J., Shanklin J. & Xu C. (2021) Mechanisms and functions of membrane lipid remodeling in plants. *The Plant Journal: for Cell and Molecular Biology*.